HRC−I Gain Correction

J. Posson−Brown, V. Kashyap (CXC/SAO)

We study the gain variations in the HRC-I over the duration of the *Chandra* mission. We analyze calibration observations of AR Lac obtained yearly at the nominal aimpoint and at 20 offset locations on the detector. We show that the gain is declining, and that the time dependence of the gain can be modeled generally as a linear decrease in PHAs. We describe the spatial and temporal characteristics of the gain decline and discuss the creation of time-dependent gain correction maps. These maps are used to convert PHAs to PI channels, thereby removing spatial and temporal dependence, and allowing source pulse-height distributions to be compared directly regardless of observation date or location on the detector.

Data

- Yearly calibration observations of AR Lac (**Table 1**) at 21 locations on the detector ($(Y_{sim}, Z_{sim}) = (0',0'), (0',\pm 2'), (\pm 2',0'), (\pm 2',\pm 2'), (0',\pm 4'), (\pm 4',0'), (0',\pm 6'), (\pm 6',0')$, and $(\pm 10',\pm 10')$). Each observation nominally 1 ks.
- Monitor gain response by tracking the median PHA over time at each of the 21 observation locations.
- Data reduced with CIAO (v3.4; CALDB v3.3), following the CIAO HRC Data Preparation analysis guide; analyzed with pre-packaged and custom-built IDL routines (e.g., `PINTofALE`).
- Background subtracted, median PHA values (and errors) estimated using Monte Carlo simulations.

Table 1: AR Lac parameters

Parameter	Value
Other Names (RA,Dec)$_{ICRS/FK5}$	HR 8448 / HD 210334 / RX J2208.6+4544 / HIP 109303 (22:08:40.818, +45:44:32.12)
$m_V, B-V$	6.13, 0.72
Distance	42 – 47 pc
Spectral Type	G2IV/K0IV (RS CVn)
M_*	3.5/3.3
Masses	$1.3/1.3\ M_\odot$
Radii	$1.8/3.1\ R_\odot$
Ephemeris	1.98316^d ; conjunction @ 2445611.6290 HJD

Characteristics of PHA Decline

- Gain decreases steadily and monotonically over time at all monitored locations (see **Figure 1**).
- Linear decrease in median PHAs (except aimpoint; linear after Dec 2000).
- Best-fit slopes roughly equal for all cases (excluding four pointings at $14.14'$ off-axis), indicating that rate of gain decline is relatively uniform across detector (see **Figure 2**).

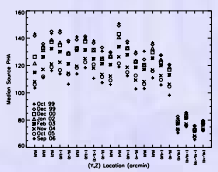

Figure 1: Median PHAs for HRC-I AR Lac observations. The background-subtracted median PHAs are plotted in a vertical row for all observations at a given location, for data obtained during different cycles, all at the low voltage setting. Data from different cycles are marked with different point types (see legend). The statistical errors on the medians are typically ≤ 1 channel. Note that the median PHAs drop monotonically.

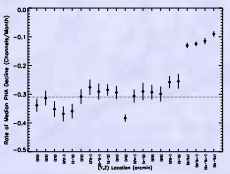

Figure 2: Uniformity of gain decline across the HRC-I. The best-fit slopes from the linear fits to the median PHAs are shown for each location. The average of the slopes (neglecting the four pointings at $14.14'$ offaxis) is shown as the dashed horizontal line. To a first approximation, excluding the far offaxis locations, the gain decline is uniform across the detector.

References

- Posson-Brown, J., Donnelly, H., 2003, *Evolution of PHA Response in the HRC* (CXC Memo, available at http://asc.harvard.edu/cal/Hrc/gain.html)
- Pease, D., Drake, J., 2003, *Monitoring the HRC-S Gain with the LETG/HRC-S* (CXC Memo, available at http://asc.harvard.edu/cal/Hrc/gain.html)
- Juda, M., 2001, *HRC Rates and High Solar Activity* (CXC Memo, available at http://hea-www.harvard.edu/~juda/memos/hrc_bkg/high_solac.html)
- Kashyap, V., Posson-Brown, J., 2005, *HRC RMF* (CXC Memo, available at http://asc.harvard.edu/cal/Hrc/RMF/index.html)
- Wilton, C., Posson-Brown, J., Juda, M., Kashyap, V., 2005 *The HRC-I Gain Map*, Poster #9.10 at the 2005 Chandra Calibration Workshop, available at http://asc.harvard.edu/cw/proceedings/05_proc/presentations/wilton/index.html
- Juda, M. et al, 2002, Proceedings of SPIE, 4851, 112

Acknowledgments

- The authors thank Michael Juda, Frank Primini, and Brad Wargelin for helpful discussions. This work was supported by NASA contract NAS8-39073 to the Chandra X-ray Center.
- Background image is from http://hea-www.harvard.edu/HRC/

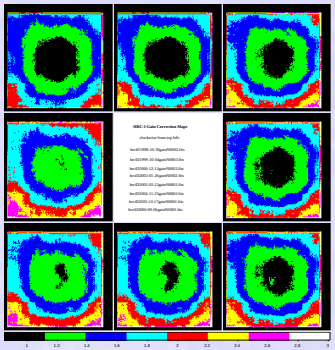

Figure 5: Gain correction maps, shown on a linear display scale from 0.85-3. The pre-flight gain correction map $g_{LAB}(\vec{x})$ is in the upper left corner. The subsequent time-dependent maps, with updates based on AR Lac observations, are shown chronologically in clockwise order.

Gain Correction

$$\begin{aligned} PI &= PHA(\vec{x},t) \times g(\vec{x}|t) \times TC(t) \\ &\equiv PHA(\vec{\theta}|t) \times TC(t) \end{aligned}$$

$$g(\vec{x}|t) = g_{LAB}(\vec{x}) \times \gamma(\vec{x}|t)$$

- $g_{LAB}(\vec{x})$: gain correction map from pre-flight ground calibration – mean of six median flat-field maps spanning 183 – 6404 eV.
- We seek to create series of gain correction maps based on lab map, preserving the high spatial-frequency information present in lab calibration data, while accounting for gross changes that have occurred in gain since launch.
- Since gain decline is linear in time and similar in rate at all monitored locations, we separate variables and compute spatial and temporal gain corrections independently.

Spatial Corrections

1. For each epoch, compute set of spatial corrective factors γ by a direct comparison of PHA spectra at each of 21 pointings to aimpoint PHA spectrum (see **Figure 3**).
2. Use γ values to interpolate minimum curvature surface at all locations over detector to obtain corrective surface $\gamma(\vec{x}|t)$. This is multiplied by high-resolution lab gain map $g_{LAB}(\vec{x})$ to obtain gain correction map $g(\vec{x}|t)$ for the epoch.
3. Test gain correction maps by independently applying $g(\vec{x}|t)$ to $PHA(\vec{x},t)$ values and comparing $median(PHA(\vec{\theta}|t))$ for all datasets. Results in **Figure 4** – medians for each epoch are uniform, i.e., gain correction has removed spatial dependence in $PHA(\vec{x},t)$.

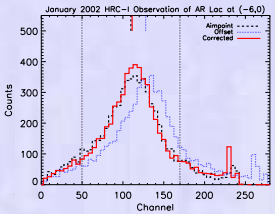

Figure 3: Matching the offset spectrum with the aimpoint spectrum to derive a corrective factor for the gain map. The figure shows the case of the spectrum from the Jan 2002 AR Lac observation at an offset pointing of $(-6',0')$ (dotted blue histogram) compared to the aimpoint spectrum (dashed black histogram). The spectra are of the quantities $g_{LAB}(\vec{x}) \cdot PHA(\vec{x},t)$. A correction factor is determined by imposing a multiplicative corrective factor on the gain until the two spectra match each other (solid red histogram; $PHA_{LAB}(\vec{x},t), \gamma = 0.875$). The matching is done over PHA values bracketed by the vertical dotted lines. Also shown on the plots as short vertical bars at the top are the locations of the medians of the spectra, in the same style as the corresponding histograms. Note that the off-axis spectra have been normalized to the same number of counts as the aimpoint spectrum.

Temporal Corrections

To find $TC(t)$:

1. Fit lines to medians of spatially-corrected PHA, i.e.

$$median(PHA(\vec{\theta}|t)) = m \cdot t + b$$

seperately for each observation location, excluding Oct and Dec 1999 data because of non-linear drop between Dec 1999 and 2000. Result is set of 21 slopes m and intercepts b.

2. Find average slope $\bar{m}$ and average intercept $\bar{b}$.
3. $\bar{b}$ corresponds to expected value of median PI for Oct 1999 if non-linear drop had not occured. To account for non-linear drop we define

$$\Delta \equiv median(PI|_{Oct99}) - \bar{b}$$

4. Finally, define

$$TC(t) = \begin{cases} \frac{\bar{b}+\Delta}{\bar{m}\,t+\bar{b}} & t > 0 \\ 1 & t = 0 \end{cases}$$

Summary

- Final *Chandra* HRC-I gain correction maps shown in **Figure 5**.
- Maps successfully remove spatial and temporal dependence in PHA as shown by AR Lac PI in **Figure 6**. Maps also tested with calibration sources HZ 43 and G21.5-0.9.
- We continue to monitor gain and investigate correlation with X-ray dosage.

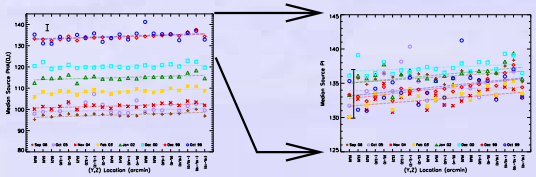

Figure 4: Median "flat-fielded" PHA values as a function of location on the detector, for all the AR Lac observations. The dashed lines show the best-fit line to each set. Since the spatial correction is relative to the aimpoint at each epoch, we expect those lines to be horizontal; the slopes of these lines are statistically indistinguishable from 0. The thick vertical line in the upper left corner shows the typical $\pm 1\sigma$ error on the medians. (Note that this is larger than the error on the raw PHA due to the uncertainty in γ, typically $\sim 1\%$.)

Figure 6: Median PI values of AR Lac datasets, calculated using the new gain correction maps, as a function of observation location. The bold vertical bar at the left shows the typical $\pm 1\sigma$ error on the medians, which includes the uncertainties in γ and $TC(t)$, typically $\sim 1\%$ and $\sim 2\%$, respectively. The horizontal dotted lines show linear least-squares fits to data for each AO. The slopes are statistically consistent with zero.